High Accuracy GPS and Antijam Protection using a P(Y) Code Digital Beamsteering Receiver

Alison Brown, *NAVSYS Corporation*

BIOGRAPHY

Alison Brown is the President and CEO of NAVSYS Corporation. She has a PhD in Mechanics, Aerospace, and Nuclear Engineering from UCLA, an MS in Aeronautics and Astronautics from MIT, and an MA in Engineering from Cambridge University. In 1986 she founded NAVSYS Corporation. Currently she is a member of the GPS-III Independent Review Team and Scientific Advisory Board for the USAF and serves on the GPS World editorial advisory board.

ABSTRACT

NAVSYS High Gain Advanced GPS Receiver (HAGR) uses a digital beam-steering antenna array to provide additional gain in the direction of the GPS satellite signals. This increases the received signal/noise ratio on the satellites tracked and also improves the accuracy of the pseudo-range and carrier-phase observations. The directivity of the digital beams created from the antenna array also reduces the effect of multipath signals and GPS jamming and interference.

This paper describes the operation of the HAGR digital beam steering array and includes test data demonstrating the high accuracy observation that it produces, Test results showing the benefits of the digital spatial processing in reducing multipath errors and GPS jamming are also included.

INTRODUCTION

A key requirement for aircraft precision approach and landing systems is to provide high quality GPS pseudo-range and carrier phase observations in both the ground reference station and the aircraft making the approach. For military applications, such as the Joint Precision Approach and Landing System (JPALS) and the Navy's Shipboard Relative GPS (SRGPS) carrier landing system, the measurement precision must be maintained in a hostile environment, where GPS jamming may occur, and also using GPS reference stations installed in less than ideal locations, for example on the mast of a ship where significant signal multipath can corrupt the measurement performance.

NAVSYS has developed a digital beam-steering GPS receiver which processes the GPS data from a multi-element phased array antenna. This has significant performance advantages over previous GPS reference station architectures which used a single reference antenna. In particular, the digital beam-steering approach has the following benefits in meeting the military JPALS or SRGPS key requirements.

1. **Must provide high accuracy pseudo-range and carrier –phase observations** The beam-steering provides gain in the direction of the GPS satellites increasing their effective C/N0Gain from beam-forming The increase in C/N0 on the GPS satellites reduces the pseudo-range and carrier-phase measurement noise improving the navigation solution accuracy.
2. **Must be able to maintain precision in the presence of close-in multipath** The digital beam-steering optimizes the adaptive antenna pattern for each satellite tracked. This provides gain in the direction of the desired satellite signal and will attenuate signals arriving from other directions, such as close-in multipath. This allows the GPS signal integrity to be maintained even under non-ideal antenna installation scenarios.
3. **Must be able to maintain performance in a jamming environment**. With conventional analog null-steering electronics, significant segments of the sky are "blanked" out when a jammer (or jammers) are detected and nulled. This will cause the GPS UE

to lose lock on multiple satellites whenever jammers are detected, reducing the satellite coverage factor. With the beam-steering approach, the antenna pattern is optimized to increase the satellite gain. This improves the satellite coverage factor increasing the availability of precision approach and landing capability in the presence of jamming

In this paper, the design of a military P(Y) code digital beam-steering GPS receiver is described and test results are included showing the receiver performance in providing high accuracy code and carrier phase observations, reducing the effect of multipath errors, and tracking the GPS satellites in the presence of a GPS jammer.

HIGH GAIN ADVANCED GPS RECEIVER

NAVSYS' High-gain Advanced GPS Receiver (HAGR)[1] was used to collect GPS measurements to observe the digital beam-steering performance in the presence of jamming. The HAGR components are illustrated in Figure 1. With the current generation analog CRPA antenna electronics in use by the DoD, a single composite RF signal is generated from the combined antenna inputs, adapted to minimize any detected jammer signals. With the HAGR digital beam-steering implementation, each antenna RF input is converted to a digital signal using a Digital Front-End (DFE). In the current HAGR configuration, up to 16 antenna elements L1 and L2 can be supported. The 16-element phased array used to support the beam-steering tests is shown in Figure 2. The HAGR can also be configured to operate with a 7-element array such as the CRPA shown in Figure 3 and the NAVSYS' 7-element Small CRPA (S-CRPA)[2].

Each DFE board in the HAGR can convert signals from four antenna elements. The digital signals from the set of the antenna inputs are then provided to the HAGR digital signal processing cards. The HAGR can be configured to track up to 12 satellites providing L1 C/A and L1 and L2 P(Y) observations when operating in the keyed mode. The digital signal processing is performed in firmware, downloaded from the host computer. Since the digital spatial processing is unique for each satellite channel, the weights can be optimized for the particular satellites being tracked. The digital architecture allows the weights to be computed in the HAGR software and then downloaded to be applied pre-correlation to create a digital adaptive antenna pattern to optimize the signal tracking performance.

DIGITAL BEAM-STEERING

The digital signal from each of the HAGR antenna elements can be described by the following equation.

$$y_k(t) = \sum_{i=1}^{Ns} s_i(\underline{x}_k, t) + n_k(t) + \sum_{k=1}^{Nj} j_j(\underline{x}_k, t)$$

where $s_i(\underline{x}_k, t)$ is the ith GPS satellite signal received at the kth antenna element

$n_k(t)$ is the noise introduced by the kth DFE

$j_j(\underline{x}_i, t)$ is the filtered jth jammer signal received at the kth antenna element

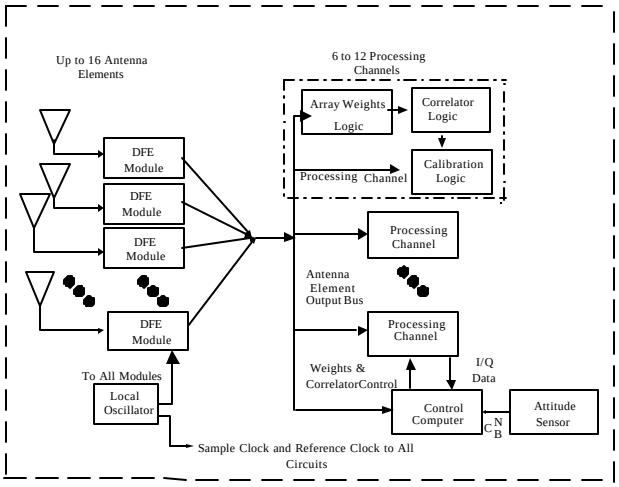

Figure 1 P(Y) HAGR System Block Diagram

Figure 2 Sixteen Element HAGR Antenna Array

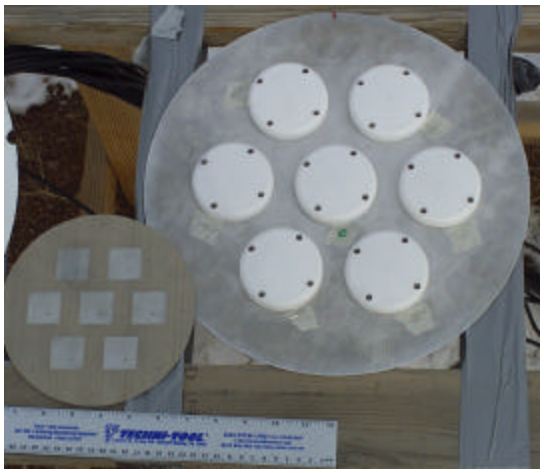

Figure 3 Seven-Element CRPA and Mini-Array

The GPS satellite signal at each antenna element ($\underline{x}_k$) can be calculated from the following equation.

$$s_i(\underline{x}_k, t) = s_i(0,t)\exp\{-i\frac{2\pi}{\lambda}\underline{1}_i^T\,\underline{x}_k) = s_i(0,t)e_{sik}$$

where $s_i(0,t)$ is the satellite signal at the array center and

$\underline{1}_i$ is the line-of-sight to that satellite

e_{sik} are the elements of a vector of phase angle offsets for satellite i to each element k

The combined digital array signal, z(t), is generated from summing the weighted individual filtered DFE signals. This can be expressed as the following equation.

$$z(t) = \underline{w}'\,\underline{y}(t) = \underline{w}'\left[\sum_{i=1}^{Ns} s_i(t)\underline{e}_{si} + \underline{n}(t) + \sum_{l=1}^{Nj} j_j(t)\underline{e}_{jl}\right]$$

With beam-steering, the optimal weights are selected to maximize the signal/noise ratio to the particular satellite being tracked. These are computed from the satellite phase angle offsets as shown in the following equation.

$$\underline{w}_{BS} = \begin{bmatrix} \exp\{-i\frac{2\pi}{\lambda}\underline{1}_i^T\,\underline{x}_1)\\ \vdots \\ \exp\{-i\frac{2\pi}{\lambda}\underline{1}_i^T\,\underline{x}_M)\end{bmatrix} = \underline{e}_s$$

In Figure 4 and Figure 5 the antenna patterns created by the digital antenna array are shown for four of the satellites tracked. The HAGR can track up to 12 satellites simultaneously. The antenna pattern provides the peak in the direction of the satellite tracked (marked 'x' in each figure). The beams follow the satellites as they move across the sky. Since the L2 wavelength is larger than the L1 wavelength, the antenna beam width is wider for the L2 antenna pattern than for the L1.

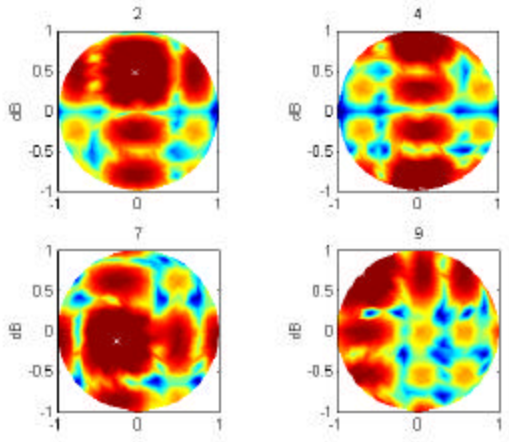

Figure 4 L1 Antenna Pattern

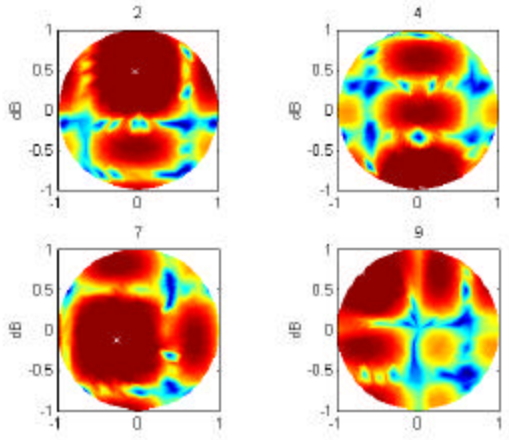

Figure 5 L2 Antenna Pattern

PSEUDO-RANGE MEASUREMENT NOISE AND MULTIPATH ERRORS

The accuracy of the HAGR pseudo-range observations is a function of the received signal strength. A data set was collected to observe the signal-to-noise ratio on the C/A and P(Y) code HAGR data over a period of 12 hours. From this data (Figure 6 and Figure 7) it can be seen that the beam-steering increases the GPS signal strength to a value of 56 dB-Hz on the C/A code. As expected the P(Y) code observed signal strength is 3 dB lower. The predicted pseudo-range noise expected at these signal strength levels is shown in Figure 11. The test data was analyzed to observe the pseudo-range noise and compare it against these predicted accuracies.

The GPS L1 pseudo-range and carrier-phase observations are described by the following equations.

$$PR_{i1}(m) = R_i + b_u + I_i + \Delta_{Ti} + \tau_{M1i} + n_{PR1}$$

$$CPH_{i1}(m) = N_1\lambda_1 + n_{CPH1} - (R_i + b_u - I_i + \Delta_{Ti} + \lambda_1\varphi_{M1i})$$

The following errors affect the pseudo-range and carrier phase observations.

1. Ionosphere errors– (I)
2. Troposphere errors – these are the same on all of the observations (Δ_{Ti})
3. Receiver Measurement Noise – these are different on each of the observations (n_{PR1} , n_{CPH1})
4. Multipath Noise – these are different on each of the observations (τ_{M1i} , $\lambda_1 \varphi_{M1i}$)
5. Satellite and Station Position error - these affect the ability to correct for the Range to the satellite (R_i)
6. Receiver clock offset (bu)

From this equation, the L1 pseudo-range + carrier phase sum cancels out the common errors and the range to the satellite and observes the pseudo-range and multipath errors as well as the change in the ionospheric offset.

$$\begin{aligned} PR_{i1} + CPH_{i1}(m) &= 2I_i + \tau_{M1i} + n_{PR1} + N_1\lambda_1 + n_{CPH1} - \lambda_1\varphi_{M1i} \\ &= C + 2I_i + \tau_{M1i} + n_{PR1} + (n_{CPH1} - \lambda_1\varphi_{M1i}) \\ &\approx C + 2I_i + \tau_{M1i} + n_{PR1} \end{aligned}$$

The PR+CPH is plotted in Figure 8 for SV 25 and each of the receiver data sets. The short term (<100 sec) white receiver noise was removed by passing the PR+CPH observation through a linear filter. The drift caused by the ionosphere on each observation was removed using a polynomial estimator. The remaining cyclic error is an estimate of the multipath pseudo-range errors. The RMS white noise on the pseudo-range observations was computed by differencing the PR+CPH measurement. This is shown in Figure 9 and Figure 10 for all of the satellites tracked for the C/A and P(Y) code observations. The observed PR noise shows good correspondence with the predicted values shown in Figure 11. For C/N0 values above 52 dB-Hz, the P(Y) code HAGR provided pseudo-range accuracies of 5 cm (1-sigma) while for C/N0 values above 55 dB-Hz the C/A code observations were accurate to 15 cm. These values are for 1-Hz observations without any carrier smoothing applied. The mean observed RMS accuracies are summarized below in Table 1 with the average peak multipath PR errors observed.

Table 1 Mean PR Noise and M-path Peak Errors (m)

SVID	C/A HAGR RMS PR	C/A Mean Mpath PR	P(Y) HAGR RMS PR	P(Y) Mean Mpath PR
1	0.239	0.259	0.054	0.202
3	0.284	0.494	0.056	0.337
8	0.200	0.278	0.045	0.202
11	0.278	0.535	0.059	0.287
13	0.252	0.321	0.059	0.260
14	0.214	0.359	0.049	0.350
20	0.222	0.267	0.050	0.164
21	0.252	0.261	0.058	0.133
22	0.248	0.318	0.047	0.217
25	0.202	0.362	0.044	0.265
27	0.183	0.270	0.044	0.178
28	0.236	0.366	0.055	0.272
29	0.225	0.312	0.050	0.217
30	0.477	0.791	0.089	0.624
31	0.325	0.266	0.055	0.135

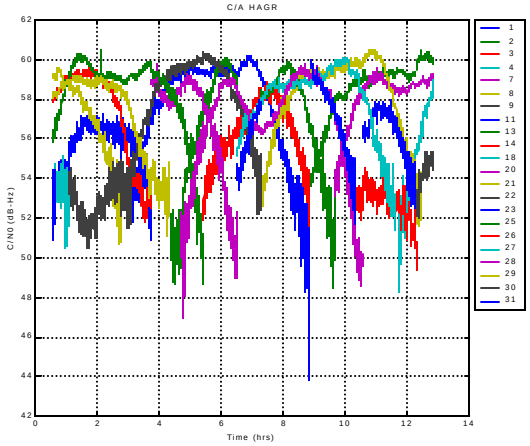

Figure 6 C/A HAGR Signal-to-Noise (dB-Hz)

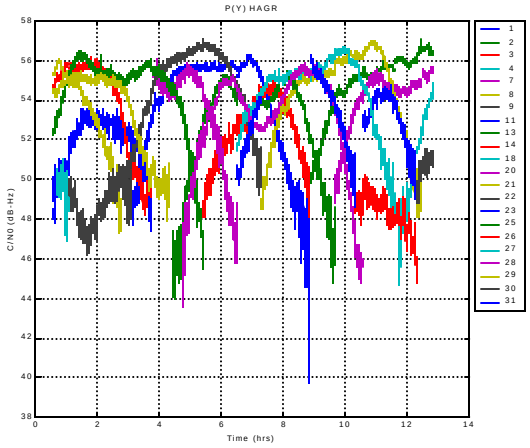

Figure 7 P(Y) HAGR Signal-to-Noise (dB-Hz)

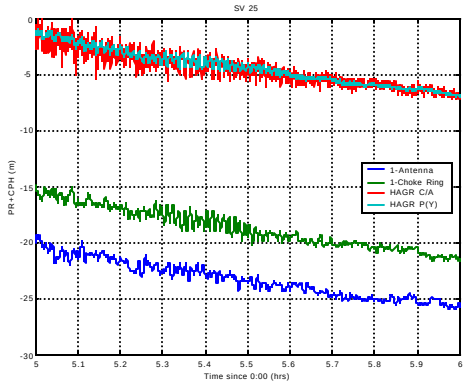

Figure 8 PR+CPH (m) - SV 25

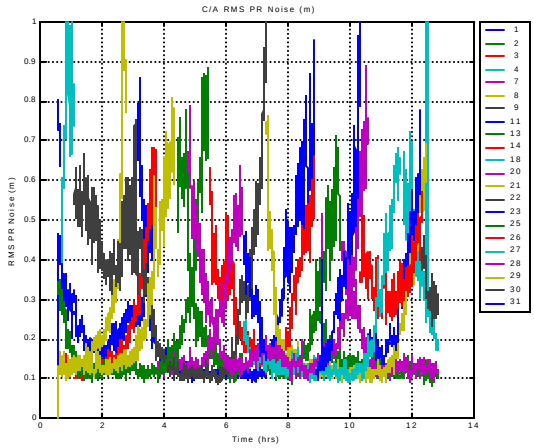

Figure 9 HAGR C/A Code Pseudo-Range Noise (m) (1-Hz DLL – no carrier smothing)

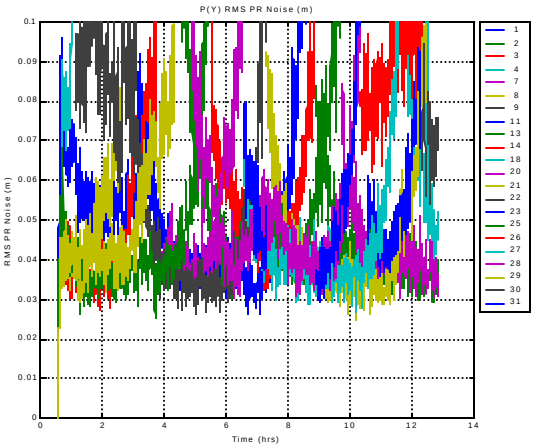

Figure 10 HAGR P(Y) Code Pseudo-Range Noise (m) (1-Hz DLL – no carrier smothing)

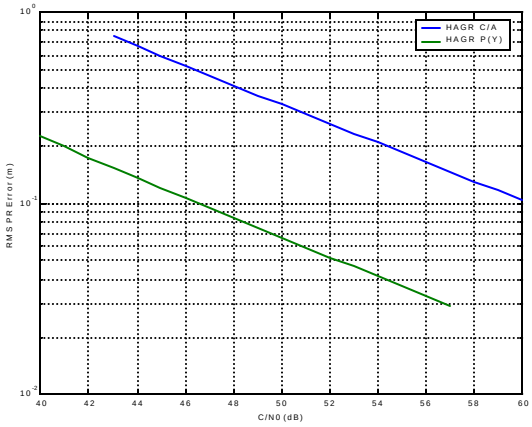

Figure 11 C/A and P(Y) HAGR RMS PR error versus C/N0

MULTIPATH REJECTION

Multipath errors are caused by the receiver tracking a composite of the direct GPS signals and reflected GPS signals from nearby objects, such as the ground or a ship's mast. Multipath errors can be observed by their effect on the measured signal/noise ratio and the code and carrier observations, as described below[3].

Signal/Noise Ratio When multipath is present the signal/noise ratio magnitude varies due to the constructive and destructive interference effect. The peak-to-peak variation is an indication of the presence of multipath signals, as shown by the following equation where A is the amplitude of the direct signal, A_M is the amplitude of the reflected multipath signal, θ is the carrier phase offset for the direct signal and θ_M is the carrier phase offset for the multipath signal.

$$\tilde{A} = \left| A + A_M e^{\Delta q} \right| - A$$

$$\tilde{q} = \angle(A + A_M e^{\Delta q})$$

$$\Delta q = q - q_M$$

The magnitude of the multipath power can be estimated from the peak-to-peak cyclic observed variation in signal/noise ratio by using the relationship plotted in Figure 12.

Carrier-phase Error The multipath carrier phase error ($\tilde{q}$) is related to the received multipath power level from the above equation. This results in a cyclic carrier phase error as the multipath signals change from constructive to destructive interference that has the peak-to-peak carrier phase error shown in Figure 13.

Pseudo-range Error For close-in multipath, where the additive delay t_M is small compared with the code chip length, the Delay Locked Loop (DLL) will converge to a value between the correct pseudo-range and the multipath pseudo-range resulting in an error that can be approximated by the following equation.

$$\tilde{t} = \frac{A_M^2}{A^2} t_M$$

The pseudo-range error that could be expected for a multipath delay of 15 m is plotted in Figure 14.

The short term cyclic variations shown in Figure 8 are caused by multipath errors. The peak-to-peak cyclic PR variation for each of the receiver data sets was calculated used to estimate the errors observed for each satellite from the pseudo-range multipath[1]. These errors are listed in Table 1 for each of the satellites.

The HAGR spatial signal processing can also be used to detect the presence of multipath and adapt the antenna pattern to further minimize these errors. A test was run to demonstrate the ability to spatially detect both the direct satellite signal and local multipath reflections. The array was placed in the parking lot at NAVSYS and tilted to deliberately assure that multipath signals would be received from the ground and near-by objects including a car located close-by (Figure 16). During the multipath

tests, data was collected using NAVSYS' Digital Storage Receiver (DSR). The DSR can be configured to record data from up to 16 independent antenna elements (see Figure 15). Post test, the data was played back from the DSR into the HAGR to perform the spatial signal processing to detect the multipath levels.

The results of this analysis for one of the satellites tracked is shown in Figure 17. The highest signal peak was detected in the direction of the satellite signal itself. From this detected line of sight direction (1_B), it was actually possible to estimate the attitude of the phased array from the known azimuth and elevation of the satellite (az_N, el_N). These are related through the body-to-nav frame direction cosine matrix, which defines the array pitch, roll and heading, through the following equation.

$$1_N(az_N, el_N) = C_B^N(PRH)1_B(az_B, el_B)$$

$$1(az, el) = \begin{bmatrix} \cos(az)\cos(el) & \sin(az)\cos(el) & \sin(el) \end{bmatrix}$$

The multipath rejection performance of the P(Y) HAGR was compared with a C/A code HAGR and also from data collected from two Novatel GPS receivers using survey antennas provided by NGS. These antennas were installed on the roof of NAVSYS' facility (Figure 18) and raw measurements were recorded over a 12-hour test window.

The signal/noise ratio from each of the receivers under test for two of the satellites tracked is shown in Figure 19 and Figure 20. When these figures are zoomed in the cyclic variation caused by the multipath constructive and destructive interference is clear (see Figure 21). The highest signal/noise ratio is observed from the C/A code measurements of the HAGR. The P(Y) code carrier-to-noise ratio (C/N0) is approximately 3 dB below this value due to the lower power of the P(Y) code signals. From Figure 21, the HAGR is applying around 11 dB of gain towards the satellite.

The peak-to-peak variation in signal/noise was computed and used to estimate the level of multipath-signal (M/S) power attenuation using the relationship shown in Figure 12. Both the C/A and P(Y) HAGR show significant attenuation of the average multipath power levels due to the beam-steering antenna pattern which gives around 10-11 dB additional multipath rejection. This will result in significantly lower carrier phase errors on the HAGR than using the conventional antennas. With an average M/S level of –6 dB the carrier phase peak multipath would be around 14 mm. With an average M/S level of –16 dB the carrier phase peak multipath error will be less than 5 mm (see Figure 13).

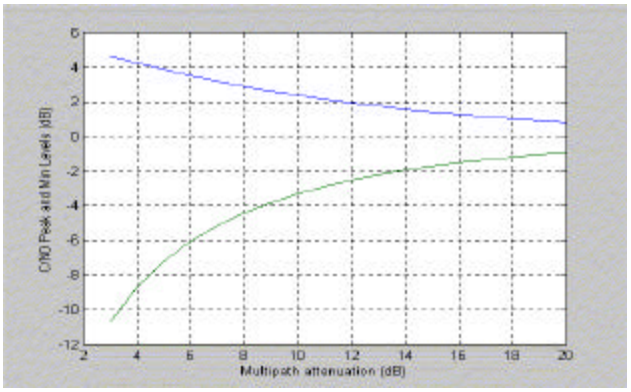

Figure 12 Multipath Amplitude Effect

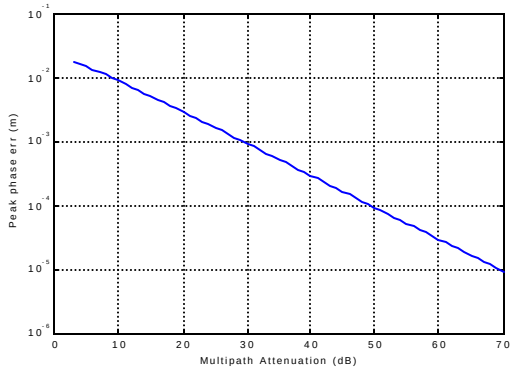

Figure 13 Multipath Peak Phase error vs. Attenuation (dB)

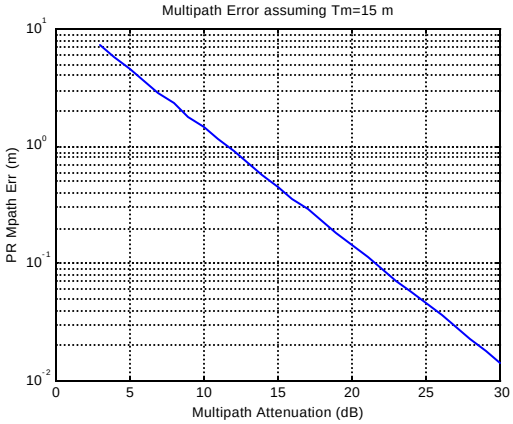

Figure 14 Peak Multipath Pseudo-Range Error

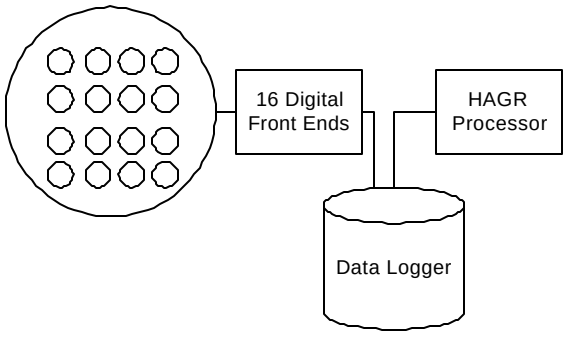

Figure 15 Sixteen Element Digital Storage Receiver

Figure 16 Multipath Array Test Set-up

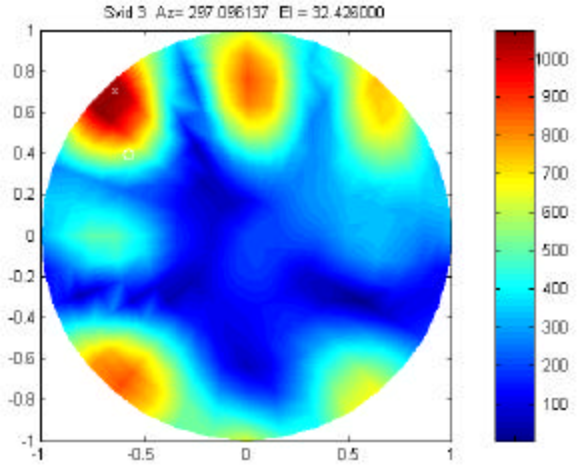

Figure 17 Detected Direct Signal and Multipath Signals from Tilted Array

Figure 18 Array Roof-Top Tests

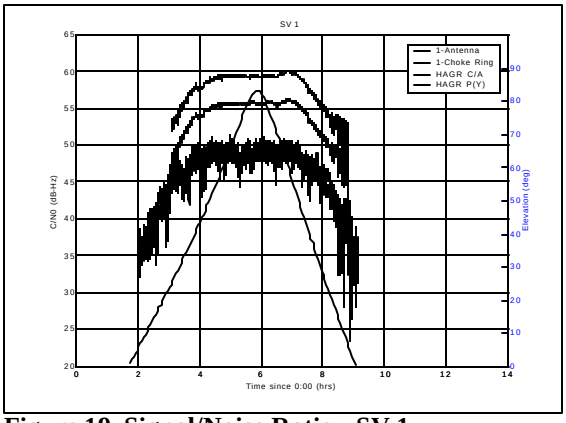

Figure 19 Signal/Noise Ratio - SV 1

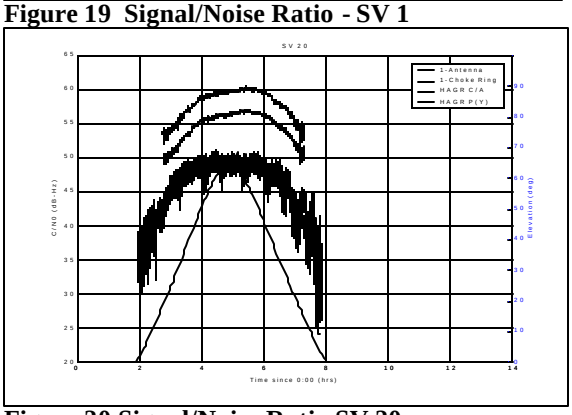

Figure 20 Signal/Noise Ratio SV 20

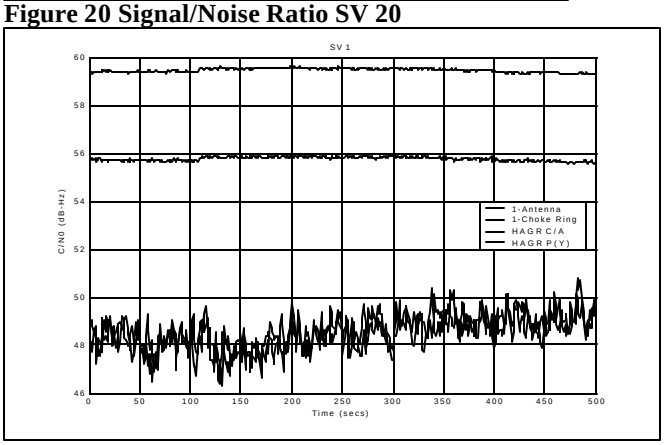

Figure 21 Signal/Noise Variation - SV 1

GPS JAMMER TESTS AND DATA COLLECTION

Jammer testing was conducted at the Army's Electronic Proving Ground (EPG) at Ft. Huachuca, Arizona[4] to evaluate the digital beaming-forming anti-jam performance. Live jamming tests were performed using a 10 MHz wide noise jammer centered at L1. A single jammer was used which was located in a mountain canyon roughly NW of the test location (see Figure 22 and Figure 23). During the tests, GPS tracking loop measurements were recorded from a 16-element HAGR antenna array (see Figure 24). The HAGR was configured to track using the L1 C/A code signals (no P(Y)), digital beam-steering. The test results collected

were compared with a SOLGR GPS receiver at the same location, which was used as a reference throughout the jammer tests.

Figure 22 is a skyplot of the satellite positions during the test, with the relative jammer position indicated by the arrow. The test site was located in a mountain canyon so many of the lower elevation satellites were masked from view. Figure 25 to Figure 28 show the HAGR C/N0 (green), the SOLGR C/N0 (blue), and the jammer to signal ratio reported by the SOLGR (red) for two of the satellites tracked. During the tests the SOLGR was reporting 40 dB to 45 dB J/S values on the L1 P(Y) code. The gain of the digital beams created from the HAGR antenna array improves the performance of the reference receiver and attenuates the jammer signals when the satellites are not in the same direction as the jammer. Further J/S performance improvements can be achieved through the use of adaptive beam-forming and null-steering using the digital spatial processing in the HAGR. The digital beam/null-steering performance is being demonstrated under an Air Force contract.

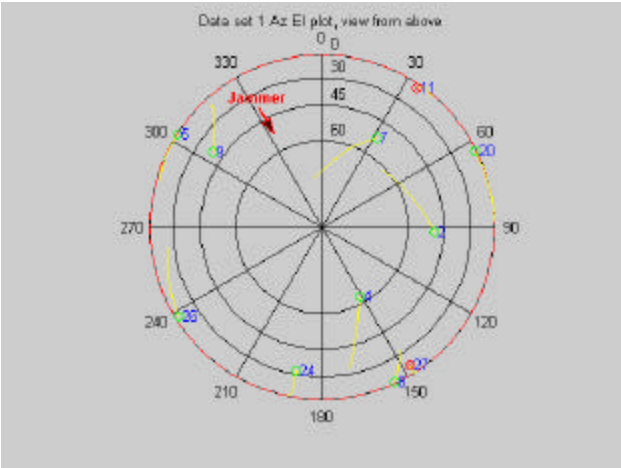

Figure 22 Satellite positions during jamming tests

Figure 23 Electronic Proving Grounds Jammer Test Site

Figure 24 HAGR at test site

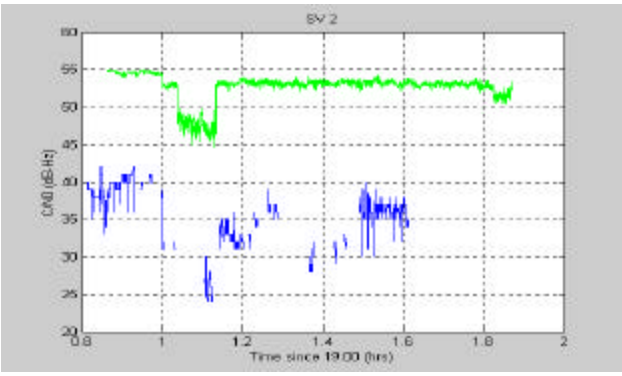

Figure 25 SV 2 C/N0

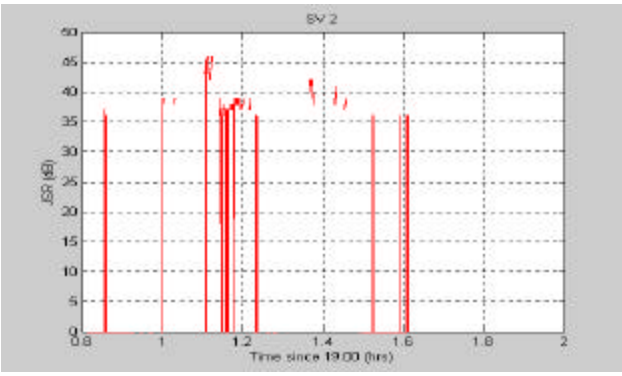

Figure 26 SV 2 SOLGR L1 P(Y) JSR

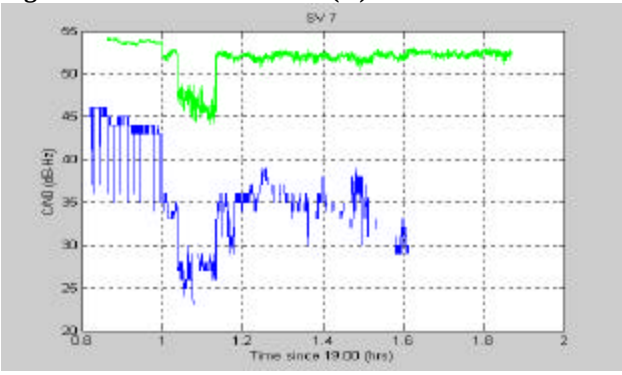

Figure 27 SV 7 C/N0

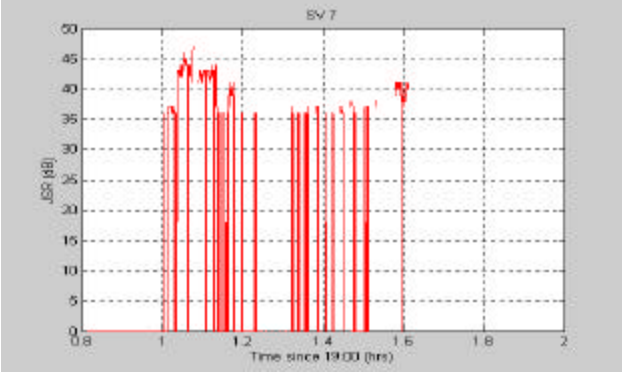

Figure 28 SV 7 SOLGR L1 P(Y) JSR

CONCLUSION

In summary, the testing has demonstrated the following advantages of the digital beam-steering P(Y) HAGR for precision GPS applications.

Beam-steering reduces the PR observation noise The digital beam-steering has the effect of increasing the observed C/N0 on all of the satellites tracked by over 10 dB when using a 16-element phased array. The test results shows that this in turn reduces the P(Y) pseudo-range noise to less than 5 cm when the C/N0 is above 52 dB-Hz.

Beam-steering reduces multipath errors The beam-steering has the effect of reducing the Multipath/Signal (M/S) relative power by 10 dB. This in turn reduces the multipath errors on the pseudo-range and carrier-phase observations. The test result showed that the peak pseudo-range error from the multipath was generally less than 30 cm. Based on our analysis, the carrier-phase multipath error should have been below 5 mm.

Beam-steering improves the Anti-Jam Performance The directivity of the beam-steering gain improves the ability of the receiver to maintain lock in the presence of a GPS jammer. Testing showed that a C/A code HAGR out performed a P(Y) code SOLGR receiver in tracking GPS satellites during a jammer trial.

The improved measurement accuracy provided by the HAGR will increase the robustness of the GPS precision solution for applications such as JPALS or SRGPS. Moreover, the high accuracy (<5 cm) pseudo-range observations will significantly reduce the length of time needed for carrier-cycle ambiguity resolution in kinematic applications. The precision observations also offer the opportunity to perform single-frequency (L1 or L2) ambiguity resolution which will increase continuity and robustness in the event of drop-outs on either the L1 or L2 signals. The use of CRPA antennas with digital beam-steering for the ground reference receivers and on-board aircraft will both improve the GPS anti-jamming performance, reduce the effect of multipath and increase the robustness and accuracy of the precision approach and landing solution for military users.

The test data presented used a digital beam-steering algorithm for the spatial processing. Currently an adaptive digital beam/null-steering version of the HAGR receiver is being developed by NAVSYS. This will be flight-tested under contract to the Air Force next year.

ACKNOWLEDGMENTS

The authors would like to acknowledge the support of the US Army Electronic Proving Ground (EPG) GPS test program for the assistance they provided during the jammer tests. The P(Y) HAGR is being developed and

tested under a contract to the US Naval Observatory (USNO). The antennas used for multipath comparison testing were provided by the National Geodetic Survey (NGS).

REFERENCES

[1] A. Brown, N. Gerein, "Test Results from a Digital P(Y) Code Beamsteering Receiver for Multipath Minimization," ION 57th Annual Meeting, Albuquerque, NM, June 2001.

[2] A. Brown and D. Morley, "Test Results Of A 7-Element Small Controlled Reception Pattern Antenna", Proceedings of ION GPS 2001, September 2001. Salt Lake City, Utah.

[3] A. Brown, "High Accuracy GPS Performance using a Digital Adaptive Antenna Array", Proceedings of ION National Technical Meeting 2001, Long Beach, CA, January 2001

[4] A. Brown and N. Gerein, "Test Results Of A Digital Beamforming GPS Receiver In A Jamming Environment", Proceedings of ION GPS 2001, September 2001. Salt Lake City, Utah